



OPEN ACCESS

EDITED BY
Bing Bai,
Beijing Jiaotong University, China

REVIEWED BY
Mingxing Zhu,
Southeast University, China
Pengpeng Ni,
Sun Yat-sen University, China

*CORRESPONDENCE
Shuaihua Ye,
yeshuaihua@163.com

SPECIALTY SECTION
This article was submitted to Structural
Materials,
a section of the journal
Frontiers in Materials

RECEIVED 07 July 2022
ACCEPTED 18 July 2022
PUBLISHED 19 September 2022

CITATION
Ma T, Zhu Y and Ye S (2022), Simplified
calculation method and stability analysis
of top beam cooperative pile–anchor
supporting slope structure.
Front. Mater. 9:988455.
doi: 10.3389/fmats.2022.988455

COPYRIGHT
© 2022 Ma, Zhu and Ye. This is an open-
access article distributed under the
terms of the [Creative Commons
Attribution License \(CC BY\)](#). The use,
distribution or reproduction in other
forums is permitted, provided the
original author(s) and the copyright
owner(s) are credited and that the
original publication in this journal is
cited, in accordance with accepted
academic practice. No use, distribution
or reproduction is permitted which does
not comply with these terms.

Simplified calculation method and stability analysis of top beam cooperative pile–anchor supporting slope structure

Tianzhong Ma^{1,2}, Yanpeng Zhu^{1,2} and Shuaihua Ye ^{1,2*}

¹Key Laboratory of Disaster Mitigation in Civil Engineering of Gansu Province, Lanzhou University of Technology, Lanzhou, China, ²Western Center of Disaster Mitigation in Civil Engineering, Ministry of Education, Lanzhou University of Technology, Lanzhou, China

Aiming at the problem of insufficient research on the action mechanism and stability calculation method of the top beam in the pile-anchor support structure, firstly the force and deformation model are established based on the elastic fulcrum method and the deformation coordination principle of the pile-anchor structure at the pile top and the anchor end in this paper. Secondly, the calculation model of the support structure under the synergy of the crown and beam and the simplified calculation method of the internal force, displacement and overall stability of the slope are constructed. Finally, combined with an engineering example, a MATLAB program was compiled for calculation, and the pile-anchor structures with crowned beams and without crowned beams were simulated and calculated by the finite element software PLAXIS 3D and Geo Studio. These three aspects are compared and verified. The results show that the internal force, deformation and minimum safety factor calculated by the method in this paper are basically consistent with the numerical simulation calculation results of the top beam condition; the existence of the top beam effectively enhances the bearing capacity of the pile body, and also restricts the displacement of the pile top development; the synergy of the crown and beam makes the safety factor of the slope increase significantly and improves the safety and stability of the slope. The research in this paper can provide a certain reference value for the theoretical calculation and design of the pile-anchor supported slope considering the top beam in engineering practice.

KEYWORDS

slope, pile-anchor support, top beam, cooperative deformation, stability

1 Introduction

As one of the main retaining structures in slope treatment, a pile–anchor supporting structure has been widely used and studied because of its strong anti-sliding ability, flexible layout, safety and reliability, less engineering quantity, and so on (Smethurst and Powrie, 2007; Kang et al., 2009; Song and Cui, 2016; Bai et al., 2019; Bai et al. 2021; Bai et al. 2022). The pile–anchor supporting structure is developed based on an ordinary

supporting pile, and it uses the elastic foundation beam theory for calculation. Furthermore, the main difference between an ordinary supporting pile and the pile–anchor supporting structure is that the former is similar to the cantilever beam structure whereas the latter can be simplified to a simply supported beam or continuous beam structure. Meanwhile, these structures are statically indeterminate structures that require simplification in the calculation (Cai and UGAI 2011; Huang et al., 2013; Chen et al., 2020).

Many scholars have studied the force and deformation of a pile–anchor supporting structure in a foundation pit and in slope engineering. Some scholars first studied the properties of soil particles and the material composition of supporting structures (Satvati et al., 2020; Zheng et al., 2021). However, the traditional design method of a pile–anchor supporting structure is mainly used to solve the problem of soil strength, and the anchor will deform with the pile in the excavation process. At this time, the existence of an anchor makes the internal force and deformation of the supporting structure more complex (Wang and Zhu, 2014; Di et al., 2018; Ye et al., 2019; Ye and Zhao., 2020). Using the strength parameters of the soil deformation state and the stress mode of a pile–anchor structure, Sun et al. (2019) established a design method for the pile–anchor structure of a deep foundation pit based on deformation. In addition, a method was proposed to unify the limit of plastic development of the soil and the checkpoint of soil deformation in a passive area of a deep foundation pit. Using limit equilibrium theory, Dong et al. (2022) established a stability model of a composite structure that considers the interaction of the anchor prestress and pile. In addition, the actual slip lines passing through the pile body, pile bottom, and soil under the pile, as well as the synergistic effect of the pile body and anchor, were further considered. Finally, the dynamic search algorithm of the model was also provided. Li and Zhang (2020) used a centrifuge test as model verification to study the development law of lateral stress and deformation of the passive pile.

Suo et al. (2016) and Wang et al. (2021) used BOTDA distributed optical fiber sensing technology to test the stress of a pile–anchor supporting system in the process of deep foundation pit excavation and studied the deformation law and internal force distribution characteristics of pile–anchor supporting structures. Furthermore, many scholars (Prat, 2017; Shu and Zhang, 2017; Zhao et al., 2018; Zhang et al., 2020) have used finite software—an indispensable research tool in geotechnical engineering—to explore pile–anchor supporting structures in slope engineering. They mainly studies the deformation and internal force of the supporting structure in the pile–anchor structure supporting slope engineering, the stability of the slope, the types and causes of anchoring failure, the influence of cutting some piles on the load transfer trend of the supporting structure, etc.

Although an existing research analysis has revealed that the research on the synergistic effect of the pile and anchor in

pile–anchor supporting structures has been mature, a top beam, which influences the deformation and internal force of the supporting pile, remains in these supporting structures (Zeng and Liu, 1995; Chen et al., 2006). Using the matrix displacement method and considering the pile–anchor as a supporting structure with a synergistic action of the pile, anchor, and soil, Ding and Zhang (2012) explored the influence of the construction process on the deformation of the supporting pile, anchor, and passive soil. Li (2011) used the method of structural mechanics to analyze the whole stress system formed by the connection of the top beam and supporting pile, and the influence of the space effect was considered. This shows that the role of top beams in pile–anchor supporting structures cannot be underestimated. However, the existing research on the theoretical research and calculation analysis of crown-beam cooperative pile–anchor slope supporting structures is relatively rare, and most of the tests consider a top beam a type of safety reserve. In addition, only a few studies have explored the deformation of crown-beam cooperative pile–anchor support in theoretical analysis, which failed to provide the theoretical calculation method of the force and deformation of the three cooperative support and the overall stability of the slope.

In this study, the mechanical models of coordinated deformation and overall stability of supporting structures, such as top beams, supporting piles, and anchors, were established using the elastic fulcrum method. A simplified calculation method was derived by considering the internal force and stability of the supporting slope with a crown-beam cooperative pile–anchor structure and was compared with numerical simulation. In addition, the cooperative action mechanism of the pile, anchor, and top beams in pile–anchor supporting structures was further studied. The important role of top beams in pile–anchor supporting structures was clarified, which can provide some theoretical guidance for designing pile–anchor supports in follow-up engineering practice.

2 Calculation of internal force and displacement

2.1 Basic assumptions

- 1) Supporting piles, top beams, and retaining plates are all linear elastomers.
- 2) The anchor rod on the side of the pile is simplified to a linear spring with horizontal stiffness.
- 3) The interaction between the pile and the surrounding soil is replaced by the soil spring, and the bonding force and friction between the pile and the soil are not considered.
- 4) The earth pressure varies linearly in the same layer of soil.

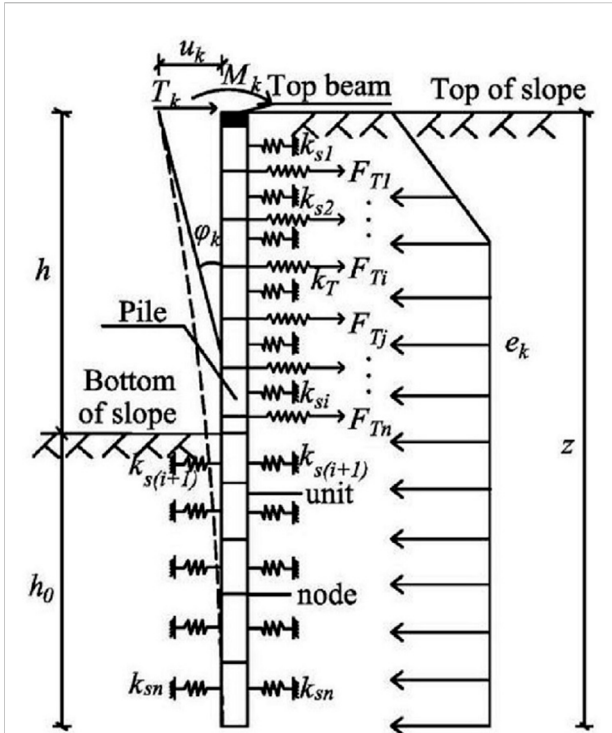


FIGURE 1 Calculation model of a single pile. Where h is the pile's length above the ground, h_0 is the embedded section's length, z is the supporting pile's full length, k_s is the equivalent stiffness of the soil spring, and k_T is the anchor's axial stiffness.

2.2 Establishment and analysis of the mechanical model

On the basis of a single pile's profile, the slope length is L , the number of piles is n , and the k th pile is inspected. The pile above the slope's bottom is considered an elastic beam constrained by a top beam and an anchor, and the pile below the slope's bottom is considered a Winkler elastic foundation beam. Figure 1 shows that the load on the k th pile is e_k and the pile top is subject to the binding T_k , the moment M_k of the top beam to the supporting pile, and the anchor tension F_{Ti} of multiple rows of anchors to the pile. Under the combined action of the above forces, the supporting pile top produces the horizontal displacement u_k and rotation angle θ_k .

2.3 Establishment of computational equations

According to the horizontal displacement u_k and rotation angle φ_k produced at the top of the k supporting pile, the horizontal displacement and rotation angle are caused by the soil pressure on the pile's side and the influence of the top beam

and anchor on the supporting pile force. In addition, some horizontal displacement and rotation angles are produced. According to the deformation coordination of the pile top beam and pile top supporting pile under the action of the anchor, to meet the superposition principle, the relationship can be written as follows:

$$\left. \begin{aligned} u_k &= u_{ek} - \delta_{ZTk}^u T_k - \delta_{ZMkk}^u M_k - \delta_{P0kFTi}^u F_{Ti} \\ \varphi_k &= \theta_{ek} - \delta_{ZTk}^\theta T_k - \delta_{ZMkk}^\theta M_k - \delta_{P0kFTi}^\theta F_{Ti} \end{aligned} \right\} \quad (1)$$

where the displacement u_{ek} and the rotation angle θ_{ek} are the horizontal displacement and rotation angle generated at the top of the k th pile under the sole action of earth pressure, respectively. δ_{ZTk}^u and δ_{ZTk}^θ are the displacement and rotation angle of the k th top in the axial direction of the vertical pile when a horizontal unit force acts on the pile top. δ_{ZMkk}^u and δ_{ZMkk}^θ are the displacement and rotation angle of the k th pile top in the vertical pile axis when the pile top has a unit external moment. δ_{P0kFTi}^u and δ_{P0kFTi}^θ are the displacement and rotation angle of the k th pile top in the vertical pile axis when the i th row of the anchor rods of the supporting pile has a horizontal unit force.

At the outer end of the anchor rod of the i th anchor rod, its horizontal displacement is caused by the joint action of the top beam and all anchor rods. According to the coordinated deformation of the anchor rod and the supporting pile under the influence of the top beam, the displacements of the outer end of the anchor rod are as follows:

$$u_{ei} - \delta_{PTk}^u T_k - \delta_{PiMk}^u M_k - \sum_{j=1}^n \delta_{PiFTj}^u F_{Tj} = \delta_{PiFTi}^u F_{Ti} \quad (i \neq j) \quad (1.2)$$

where the pile body produces a horizontal displacement u_{ei} under the sole action of earth pressure, δ_{PTk}^u and δ_{PiMk}^u are the displacements of the horizontal unit force and unit moment acting on the outer end of the i th row of the anchor rods on the k th pile top, respectively, δ_{PiFTj}^u is the displacement of the unit axial force of the anchor rod of the j th row of the supporting pile acting on the outer end of the anchor rod of the i th row of the pile, and δ_{PiFTi}^u is the displacement of the unit axial force of the i th row of the anchor rods of the supporting piles acting on the outer ends of the anchor rods of this row.

2.4 Solutions of equation parameters

In Eq. 1, the calculation ideas of u_{ek} , θ_{ek} , δ_{ZTk}^u , δ_{ZTk}^θ , δ_{ZMkk}^u , δ_{ZMkk}^θ , δ_{P0kFTi}^u and δ_{P0kFTi}^θ are as follows:

2.4.1 Finite element of a structure

The vertical supporting pile is divided into a limited number of elements, and one element is divided every 1–3 m. To facilitate calculation, the nodes on the boundary are used to connect the elements in the cross section of the supporting structure, the action point of the anchor, the sudden change in load, and so on.

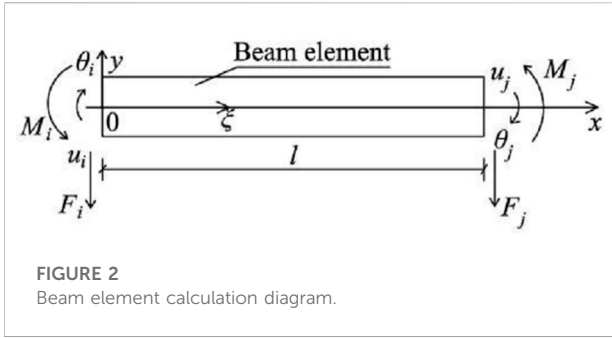


FIGURE 2
Beam element calculation diagram.

On the basis of the principle of no relative displacement in the coordination of the supporting pile, anchor bar, top beam, and soil, the soil stiffness of the element length is equivalent to soil spring k_{si} . The anchor force is F_{Ti} , and the bolt stiffness is k_{Ti} (Figure 1).

2.4.2 Application of the matrix displacement method

The element node load and the element stiffness matrix are generally calculated using the shape function of the compression bar element (Figure 2).

The interpolation of the deflection function $y(\xi)$ in the element is shown below.

$$y(\xi) = \sum_{i=1}^4 N_i(\xi) \alpha^e \tag{2}$$

In the formula: $N_i = [N_1 \ N_2 \ N_3 \ N_4]$; $N_1(\xi) \sim N_4(\xi)$ is the shape function simplified as follows: $N_1 = 1 - 3\xi^2 + 2\xi^3$, $N_2 = (\xi - 2\xi^2 + \xi^3)l$, $N_3 = 3\xi^2 - 2\xi^3$, and $N_4 = (\xi^3 - \xi^2)l$; $\alpha^e = [u_i \ \theta_i \ u_j \ \theta_j]^T$, where u_i is the linear displacement, θ_i is the angular displacement, $\theta_i = (\frac{dy}{dx})_i$, $\xi = \frac{x}{l}$ ($0 \leq \xi \leq 1$), and ξ is a certain point in the unit.

2.4.2.1 Joint load of elements

The main loads acting on the supporting pile are the force of the top beam on the supporting pile, the pulling force of the anchor on the supporting pile, and the earth pressure behind the supporting pile, in which the acting force of the top beam on the supporting pile and the pulling force of the anchor on the supporting pile belong to the nodal load. The earth pressure behind the pile belongs to the non-nodal load. According to the calculation rules of the matrix finite element method, the non-nodal load of the earth pressure behind the pile should be transformed into the equivalent nodal load. Therefore, the load concentration degree of the earth pressure behind the pile is assumed to be $p(x)$, and the equivalent nodal load of the load concentration $p(x)$ in the local coordinate system of element node i and node j is as follows:

$$\begin{aligned} \{F_P\}^e &= \begin{Bmatrix} F_i \\ M_i \\ F_j \\ M_j \end{Bmatrix} = \int_0^l [N]^T b_0 p(\xi) l d\xi \\ &= b_0 l \begin{Bmatrix} \int_0^1 N_1(\xi) p(\xi) d\xi \\ \int_0^1 N_2(\xi) p(\xi) d\xi \\ \int_0^1 N_3(\xi) p(\xi) d\xi \\ \int_0^1 N_4(\xi) p(\xi) d\xi \end{Bmatrix} \end{aligned} \tag{3}$$

where b_0 is the beam element width, $p(\xi)$ is the load concentration, l is the element length, F_i is the horizontal load of node i , and M_i is the moment of node i .

When the earth pressure varies linearly in the same soil layer, there are

$$p(\xi) = p_i + (p_j - p_i)\xi \tag{4}$$

By integrating Eq. 4 into Eq. 3, the equivalent joint load caused by earth pressure is as follows:

$$\{F_P\}^e = \begin{Bmatrix} F_i \\ M_i \\ F_j \\ M_j \end{Bmatrix} = b_0 p_i l \begin{Bmatrix} 1/2 \\ l_{12} \\ 1/2 \\ -l_{12} \end{Bmatrix} + b_0 (p_j - p_i) l \begin{Bmatrix} 3/20 \\ l_{30} \\ 7/20 \\ -l_{20} \end{Bmatrix} \tag{5}$$

2.4.2.2 Element stiffness matrix

From the analysis of the supporting pile, the element stiffness matrix comprises three parts: the first is the stiffness $[k_P]^e$ of the row pile, the second is the equivalent stiffness $[k_s]^e$ produced by the soil of the element length, and the third is the anchor axial stiffness $[k_T]^e$. The stiffness $[k]^e$ of the element in the global coordinate system is as follows:

$$[k]^e = [k_P]^e + [k_s]^e + [k_T]^e \tag{6}$$

The element stiffness $[k_P]^e$ of row piles is as follows:

$$[k_P]^e = \frac{EI}{l^3} \begin{bmatrix} 12 & 6l & -12 & 6l \\ 6l & 4l^2 & -6l & 2l^2 \\ -12 & -6l & 12 & -6l \\ 6l & 2l^2 & -6l & 4l^2 \end{bmatrix} \tag{7}$$

where E is the elastic modulus of the pile, I is the moment of inertia of the pile section, and l is the element length.

According to the beam model of the elastic foundation, the following results can be obtained:

$$p(z) = mzw(z) \tag{8}$$

where $p(z)$ is the pressure strength of any point on the pile, $w(z)$ is the horizontal displacement of the pile, m is the horizontal elastic coefficient of the foundation, and z is the pile length.

Eq. 8 can be substituted into Eq. 3 to obtain:

$$\{F_p\}^e = \int_0^l [N]^T b_0 p(\xi) d\xi = b_0 l \int_0^1 m z [N] d\xi \{a^e\} \quad (9.1)$$

$$[k_s]^e = b_0 l \int_0^1 m z [N]^T [N] d\xi \quad (9.2)$$

Through integration, the equivalent stiffness e_{sk} produced by the soil of the element can be obtained as follows:

$$[k_s]^e = m z b_0 l \begin{bmatrix} \frac{13}{25} & \frac{11}{210}l & \frac{9}{70} & -\frac{13}{420}l \\ \frac{11}{210}l & \frac{1}{105}l^2 & \frac{13}{420}l & -\frac{1}{140}l^2 \\ \frac{9}{70} & \frac{13}{420}l & \frac{13}{25} & -\frac{11}{210}l \\ -\frac{13}{420}l & -\frac{1}{140}l^2 & -\frac{11}{210}l & \frac{1}{105}l^2 \end{bmatrix} \quad (10)$$

where M is the horizontal elastic coefficient of the foundation, l is the element length, and b_0 is the width of the beam element.

The stiffness $[k_T]^e$ of the anchor element is as follows:

$$[k_T]^e = \frac{EA}{l_i} \begin{bmatrix} 1 & 0 & -1 & 0 \\ 0 & 0 & 0 & 0 \\ -1 & 0 & 1 & 0 \\ 0 & 0 & 0 & 0 \end{bmatrix} \quad (11)$$

where E is the elastic modulus of the bolt, A is the cross-sectional area of the bolt, and l_i is the bolt length.

2.4.3 Establishing the equilibrium equation

The overall stiffness matrix of the structure is obtained by transforming several element stiffness matrixes, and the following formula can be obtained according to the matrix displacement method:

$$[k]\{\delta\} = \{F\} \quad (12)$$

where $[k]$ is the overall stiffness matrix, $\{\delta\}$ is the overall nodal displacement matrix, and $\{F\}$ is the overall load matrix.

2.4.4 Solving the equilibrium equation

From Eq. 12, it can be obtained that the horizontal displacement u_{ek} and rotation angle θ_{ek} of the k th pile top are produced by the supporting pile under the action of earth pressure alone, and when the horizontal unit force and unit external moment act separately on the k th pile top, the vertical pile axis displacements δ_{ZTkk}^u and δ_{ZTkk}^θ and rotation angles δ_{ZMkk}^u and δ_{ZMkk}^θ occur at the pile top. Using the method of structural mechanics, the flexibility coefficients δ_{P0kFTi}^u and δ_{P0kFTi}^θ at the pile top can be obtained when the row anchor i has a horizontal unit force.

$$\left. \begin{aligned} u_k &= \sum_{m=1}^n \delta_{LFkm}^u \cdot T_m \\ \varphi_k &= \sum_{m=1}^n \delta_{LMkm}^\theta \cdot M_m \end{aligned} \right\} \quad (13)$$

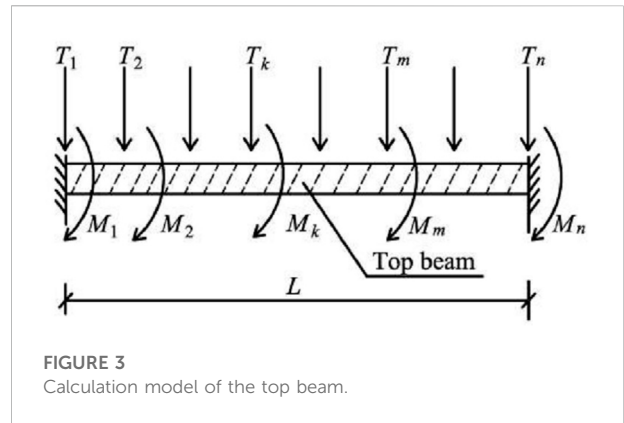


FIGURE 3 Calculation model of the top beam.

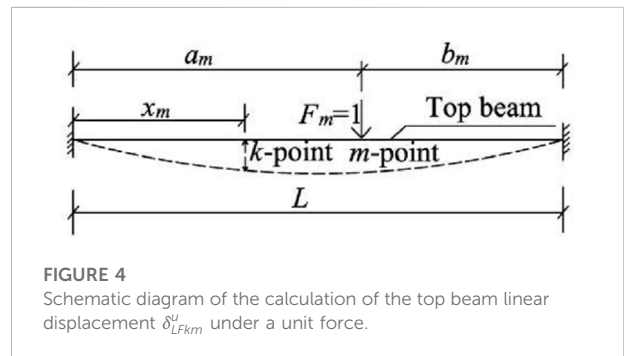


FIGURE 4 Schematic diagram of the calculation of the top beam linear displacement δ_{LFkm}^u under a unit force.

$$\delta_{LFkm}^u = \frac{b_m^2 x_k^2}{6EIL^2} \left[3a_m - \left(1 + \frac{2a_m}{L} \right) x_m \right] \quad (k \leq m) \quad (14)$$

2.5 Displacement and rotation angle at the k th pile top under the action of the top beam

The top beam can be considered a linear elastic body. On the basis of the analysis of the top beam of the supporting pile, the two ends of the top beam are assumed to be fixed-end constraints (Figure 3), where the length of the top beam is L , the n supporting piles connected to the horizontal force of the top beam have $T_1, T_2, T_3, \dots, T_n$ and the bending moments produced by the top beam are $M_1, M_2, M_3, \dots, M_n$. Considering the k th pile top on the top beam for analysis, according to the superposition principle, the displacement u_k and rotation angle φ_k of the k th pile on the top beam can be obtained. where δ_{LFkm}^u is the displacement of the top beam at the k th point when the unit horizontal force at the m th point acts alone and δ_{LMkm}^θ is the rotation angle of the top beam at the k th point when the unit bending moment at the m th point acts alone.

2.5.1 Calculation of the related parameter δ_{LFkm}^u in the top beam calculation formula

Figure 4 shows that when the unit force is applied to a top beam with fixed-end constraints at both ends, the parameter δ_{LFkm}^u beam can be derived from the knowledge of structural mechanics. where a_m, b_m, x_k , and L have their usual meanings, as in Figure 4, E is the

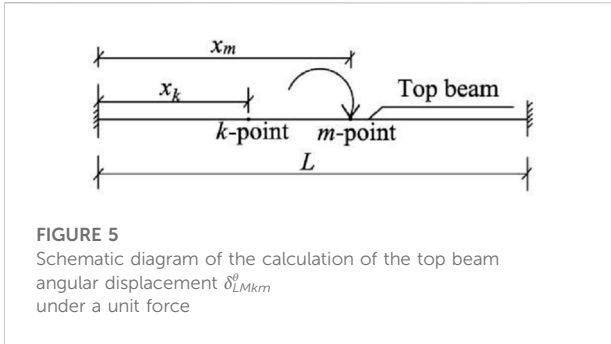


FIGURE 5
Schematic diagram of the calculation of the top beam angular displacement δ_{LMkm}^θ under a unit force

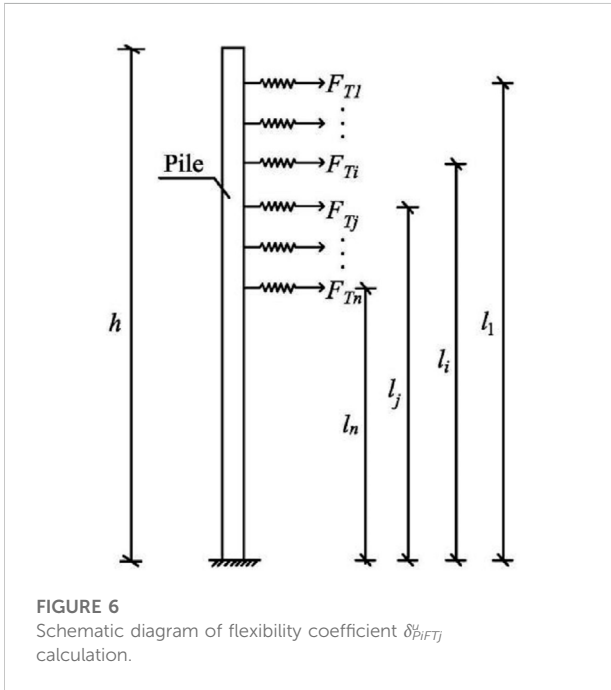


FIGURE 6
Schematic diagram of flexibility coefficient δ_{PiFTj}^u calculation.

elastic modulus of the top beam, and I is the section moment of inertia of the top beam.

2.5.2 Calculation of the related parameter δ_{LMkm}^θ in the top beam calculation formula

According to the principle of material mechanics, the equation for the parameter δ_{LMkm}^θ can be derived. As shown in Figure 5, the calculation formula of the δ_{LMkm}^θ equation is shown in Eq. 15. where G is the shear modulus of the top beam, I_t is the polar moment of inertia of the top beam, L is the length of the top beam, a is the calculation factor of the top beam's polar moment of inertia, and b is the short side of the section of the top beam rectangle.

2.6 Displacement of the outer end of the i th anchor under the action of the top beam

The horizontal displacement at the anchor end of the i -row anchor under the influence of the top beam is consistent with the deformation of the anchor rod and supporting pile.

$$\left. \begin{aligned} \delta_{LMkm}^\theta &= \frac{(L - x_m) \cdot x_k}{GI_t L} \quad (k \leq m) \\ I_t &= ab^4 \end{aligned} \right\} \quad (15)$$

$$u_{ei} - \delta_{PiT_k}^u \cdot T_k - \delta_{PiM_k}^u \cdot M_k - \sum_{j=1}^n \delta_{PiFT_j}^u \cdot F_{Tj} = \delta_{PiFT_i}^u \cdot F_{Ti} \quad (i \neq j) \quad (16)$$

where the horizontal displacement of the pile is u_{ei} under the action of earth pressure alone. The displacements of the horizontal unit force and the unit moment acting on the k th pile top are, respectively, the displacements of the horizontal unit force and the unit moment acting on the anchor end of the i -row of the pile, the $\delta_{PiFT_j}^u$ pile is the displacement of the j th row anchor unit axial force acting on the i -row anchor end of the pile, and the $\delta_{PiFT_i}^u$ anchor is the displacement of the i th row anchor unit axial force acting on the anchor end of the supporting pile.

Assuming that the pile bottom is the fixed end, the height of the anchor action point to the supporting pile bottom is l_i , and the component of the anchor tension in the horizontal direction is F_{Ti} , the flexibility coefficients of $\delta_{PiT_k}^u$, $\delta_{PiM_k}^u$, $\delta_{PiFT_j}^u$ and $\delta_{PiFT_i}^u$ can be obtained according to the method of structural mechanics. For example, Figure 6 shows the calculation of the $\delta_{PiFT_j}^u$ flexibility coefficient. where E is the elastic modulus of the supporting pile, I is the moment of inertia of the supporting pile section, and l_i , l_j are the heights from the point of action of the i th and j th rows of the anchor rods to the bottom of the supporting pile.

$$\delta_{PiFT_j}^u = \frac{l_j^2}{6EI} (3l_i - l_j) \quad (i = 1 \sim n, j = 1 \sim n) \quad (17)$$

Simultaneously, Eqs 1, 16 can be used to solve 3n unknown quantities, namely, T_k , M_k , and F_{Ti} ($i \neq j$).

2.7 Calculating the force between the pile top and anchor end

According to the coordinated deformation of the pile-anchor structure at the top of the pile and the end of the anchor:

$$\begin{cases} u_{ek} - \delta_{ZTkk}^\theta T_k - \delta_{ZMkk}^\theta M_k - \delta_{p0kF_{Ti}}^u F_{Ti} = \sum_{m=1}^n \delta_{LFkm}^u T_m \\ \theta_{ek} - \delta_{ZTkk}^\theta T_k - \delta_{ZMkk}^\theta M_k - \delta_{p0kF_{Ti}}^\theta F_{Ti} = \sum_{m=1}^n \delta_{LMkm}^\theta M_m \\ u_{ei} - \delta_{PiT_k}^u T_k - \delta_{PiM_k}^u M_k - \sum_{j=1}^n \delta_{PiFT_j}^u F_{Tj} = \delta_{PiFT_i}^u F_{Ti} \end{cases} \quad (18)$$

It can be simplified to a system of linear equations in three variables:

$$\begin{cases} a_1 x_1 + b_1 x_2 + c_1 x_3 = d_1 \\ a_2 x_1 + b_2 x_2 + c_2 x_3 = d_2 \\ a_3 x_1 + b_3 x_2 + c_3 x_3 = d_3 \end{cases} \quad (19)$$

Among them:

$$\begin{aligned}
 a_1 &= \begin{bmatrix} \delta_{LF11}^u + \delta_{ZF11}^u & \dots & \delta_{LF1k}^u & \delta_{LF1m}^u & \dots & \delta_{LF1n}^u \\ \dots & \dots & \dots & \dots & \dots & \dots \\ \delta_{LFk1}^u & \dots & \delta_{LFkk}^u + \delta_{ZFkk}^u & \delta_{LFkm}^u & \dots & \delta_{LFkn}^u \\ \delta_{LFm1}^u & \dots & \delta_{LFmk}^u & \delta_{LFmm}^u + \delta_{ZFmm}^u & \dots & \delta_{LFmn}^u \\ \dots & \dots & \dots & \dots & \dots & \dots \\ \delta_{LFn1}^u & \dots & \delta_{LFnk}^u & \delta_{LFnm}^u & \dots & \delta_{LFnn}^u + \delta_{ZFnn}^u \end{bmatrix}, \\
 b_1 &= \begin{bmatrix} \delta_{LM11}^u & \dots & \delta_{LM1k}^u & \delta_{LM1m}^u & \dots & \delta_{LM1n}^u \\ \dots & \dots & \dots & \dots & \dots & \dots \\ \delta_{LMk1}^u & \dots & \delta_{LMkk}^u & \delta_{LMkm}^u & \dots & \delta_{LMkn}^u \\ \delta_{LMm1}^u & \dots & \delta_{LMmk}^u & \delta_{LMmm}^u & \dots & \delta_{LMmn}^u \\ \dots & \dots & \dots & \dots & \dots & \dots \\ \delta_{LMn1}^u & \dots & \delta_{LMnk}^u & \delta_{LMnm}^u & \dots & \delta_{LMnn}^u \end{bmatrix}, \\
 c_1 &= \begin{bmatrix} \delta_{P0_1F_{T1}}^u & \dots & \delta_{P0_1F_{Ti}}^u & \delta_{P0_1F_{Tj}}^u & \dots & \delta_{P0_1F_{Tn}}^u \\ \dots & \dots & \dots & \dots & \dots & \dots \\ \delta_{P0_iF_{T1}}^u & \dots & \delta_{P0_iF_{Ti}}^u & \delta_{P0_iF_{Tj}}^u & \dots & \delta_{P0_iF_{Tn}}^u \\ \delta_{P0_jF_{T1}}^u & \dots & \delta_{P0_jF_{Ti}}^u & \delta_{P0_jF_{Tj}}^u & \dots & \delta_{P0_jF_{Tn}}^u \\ \dots & \dots & \dots & \dots & \dots & \dots \\ \delta_{P0_nF_{T1}}^u & \dots & \delta_{P0_nF_{Ti}}^u & \delta_{P0_nF_{Tj}}^u & \dots & \delta_{P0_nF_{Tn}}^u \end{bmatrix}, \\
 a_2 &= \begin{bmatrix} \delta_{LF11}^\theta & \dots & \delta_{LF1k}^\theta & \delta_{LF1m}^\theta & \dots & \delta_{LF1n}^\theta \\ \dots & \dots & \dots & \dots & \dots & \dots \\ \delta_{LFk1}^\theta & \dots & \delta_{LFkk}^\theta & \delta_{LFkm}^\theta & \dots & \delta_{LFkn}^\theta \\ \delta_{LFm1}^\theta & \dots & \delta_{LFmk}^\theta & \delta_{LFmm}^\theta & \dots & \delta_{LFmn}^\theta \\ \dots & \dots & \dots & \dots & \dots & \dots \\ \delta_{LFn1}^\theta & \dots & \delta_{LFnk}^\theta & \delta_{LFnm}^\theta & \dots & \delta_{LFnn}^\theta \end{bmatrix}, \\
 b_2 &= \begin{bmatrix} \delta_{LM11}^\theta + \delta_{ZM11}^\theta & \dots & \delta_{LM1k}^\theta & \delta_{LM1m}^\theta & \dots & \delta_{LM1n}^\theta \\ \dots & \dots & \dots & \dots & \dots & \dots \\ \delta_{LMk1}^\theta & \dots & \delta_{LMkk}^\theta + \delta_{ZMkk}^\theta & \delta_{LMkm}^\theta & \dots & \delta_{LMkn}^\theta \\ \delta_{LMm1}^\theta & \dots & \delta_{LMmk}^\theta & \delta_{LMmm}^\theta + \delta_{ZMmm}^\theta & \dots & \delta_{LMmn}^\theta \\ \dots & \dots & \dots & \dots & \dots & \dots \\ \delta_{LMn1}^\theta & \dots & \delta_{LMnk}^\theta & \delta_{LMnm}^\theta & \dots & \delta_{LMnn}^\theta + \delta_{ZMnn}^\theta \end{bmatrix}, \\
 c_2 &= \begin{bmatrix} \delta_{P0_1F_{T1}}^\theta & \dots & \delta_{P0_1F_{Ti}}^\theta & \delta_{P0_1F_{Tj}}^\theta & \dots & \delta_{P0_1F_{Tn}}^\theta \\ \dots & \dots & \dots & \dots & \dots & \dots \\ \delta_{P0_iF_{T1}}^\theta & \dots & \delta_{P0_iF_{Ti}}^\theta & \delta_{P0_iF_{Tj}}^\theta & \dots & \delta_{P0_iF_{Tn}}^\theta \\ \delta_{P0_jF_{T1}}^\theta & \dots & \delta_{P0_jF_{Ti}}^\theta & \delta_{P0_jF_{Tj}}^\theta & \dots & \delta_{P0_jF_{Tn}}^\theta \\ \dots & \dots & \dots & \dots & \dots & \dots \\ \delta_{P0_nF_{T1}}^\theta & \dots & \delta_{P0_nF_{Ti}}^\theta & \delta_{P0_nF_{Tj}}^\theta & \dots & \delta_{P0_nF_{Tn}}^\theta \end{bmatrix}, \\
 a_3 &= \begin{bmatrix} \delta_{P1T_1}^u & \dots & \delta_{P1T_k}^u & \delta_{P1T_m}^u & \dots & \delta_{P1T_n}^u \\ \dots & \dots & \dots & \dots & \dots & \dots \\ \delta_{PiT_1}^u & \dots & \delta_{PiT_k}^u & \delta_{PiT_m}^u & \dots & \delta_{PiT_n}^u \\ \delta_{PjT_1}^u & \dots & \delta_{PjT_k}^u & \delta_{PjT_m}^u & \dots & \delta_{PjT_n}^u \\ \dots & \dots & \dots & \dots & \dots & \dots \\ \delta_{PnT_1}^u & \dots & \delta_{PnT_k}^u & \delta_{PnT_m}^u & \dots & \delta_{PnT_n}^u \end{bmatrix}, \\
 b_3 &= \begin{bmatrix} \delta_{P1M_1}^u & \dots & \delta_{P1M_k}^u & \delta_{P1M_m}^u & \dots & \delta_{P1M_n}^u \\ \dots & \dots & \dots & \dots & \dots & \dots \\ \delta_{PiM_1}^u & \dots & \delta_{PiM_k}^u & \delta_{PiM_m}^u & \dots & \delta_{PiM_n}^u \\ \delta_{PjM_1}^u & \dots & \delta_{PjM_k}^u & \delta_{PjM_m}^u & \dots & \delta_{PjM_n}^u \\ \dots & \dots & \dots & \dots & \dots & \dots \\ \delta_{PnM_1}^u & \dots & \delta_{PnM_k}^u & \delta_{PnM_m}^u & \dots & \delta_{PnM_n}^u \end{bmatrix}, \\
 c_3 &= \begin{bmatrix} \delta_{P1F_{T1}}^u & \dots & \delta_{P1F_{Ti}}^u & \delta_{P1F_{Tj}}^u & \dots & \delta_{P1F_{Tn}}^u \\ \dots & \dots & \dots & \dots & \dots & \dots \\ \delta_{PiF_{T1}}^u & \dots & \delta_{PiF_{Ti}}^u & \delta_{PiF_{Tj}}^u & \dots & \delta_{PiF_{Tn}}^u \\ \delta_{PjF_{T1}}^u & \dots & \delta_{PjF_{Ti}}^u & \delta_{PjF_{Tj}}^u & \dots & \delta_{PjF_{Tn}}^u \\ \dots & \dots & \dots & \dots & \dots & \dots \\ \delta_{PnF_{T1}}^u & \dots & \delta_{PnF_{Ti}}^u & \delta_{PnF_{Tj}}^u & \dots & \delta_{PnF_{Tn}}^u \end{bmatrix},
 \end{aligned}$$

$$\begin{aligned}
 x_1 &= \begin{bmatrix} T_1 \\ \dots \\ T_k \\ \dots \\ T_m \\ \dots \\ T_n \end{bmatrix}, x_2 = \begin{bmatrix} M_1 \\ \dots \\ M_k \\ \dots \\ M_m \\ \dots \\ M_n \end{bmatrix}, x_3 = \begin{bmatrix} F_{T_1} \\ \dots \\ F_{T_i} \\ \dots \\ F_{T_j} \\ \dots \\ F_{T_n} \end{bmatrix}, d_1 = \begin{bmatrix} u_{e1} \\ \dots \\ u_{ek} \\ \dots \\ u_{em} \\ \dots \\ u_{en} \end{bmatrix}, \\
 d_2 &= \begin{bmatrix} \theta_{e1} \\ \dots \\ \theta_{ek} \\ \dots \\ \theta_{em} \\ \dots \\ \theta_{en} \end{bmatrix}, d_3 = \begin{bmatrix} u_{e1} \\ \dots \\ u_{ei} \\ \dots \\ u_{ej} \\ \dots \\ u_{en} \end{bmatrix}
 \end{aligned}$$

To solve Eq. 19, it can be got 3n unknowns, namely, T_k , M_k , and F_{T_i} ($k = i = 1, 2, \dots, n$).

2.8 Solving the internal force and displacement of the supporting pile

Taking the k th supporting pile as the research object, the loads acting on the supporting pile include the force T_k and moment M_k of method of the top beam on the supporting pile, the earth pressure e_k , and the anchor tension F_{T_i} . The finite elementthe beam system on an elastic foundation is selected to solve the internal force and deformation of the k th root supporting pile. The structural equilibrium equation is as follows:

$$[k] \begin{Bmatrix} u_i \\ \theta_i \\ u_j \\ \theta_j \end{Bmatrix} = \begin{Bmatrix} F_i \\ M_i \\ F_j \\ M_j \end{Bmatrix} \quad (i = 1 \sim n, j = 1 \sim n) \quad (20)$$

where $[k]$ is the element stiffness matrix in the global coordinate system, u_i is the linear displacement of node i , and θ_i is the angular displacement of node i .

3 Stability analysis of a slope supported by a top beam combined with a pile and an anchor

3.1 Basic assumptions

- 1) The form of the slip surface is a circular arc when the whole support system is unstable.
- 2) The sliding soil zone in the arc is divided into several vertical soil strips, the interaction between the soil strips is ignored, and the arc at the lower end of the soil strip is approximately replaced by a straight line.
- 3) The shear strength on the slip surface is determined by the Mohr-Coulomb failure criterion.

- 4) For the pile–anchor supporting system, when the slip surface passes through the anchor and the supporting pile, the supporting structure will provide tensile moment and anti-sliding moment.
- 5) Search all arc surfaces that may pass through the bottom of the pile and below, and the most dangerous slip surface is the arc surface with the minimum safety factor.

3.2 Establishment of the calculation model

On the basis of the Swedish slice method, without considering the interaction between the two sides of the soil strip, the sliding part of the slope is divided into several soil strips, and the width of the strip b_i is 0.5 m. Taking the point of the top surface of the top beam (corresponding to the pile center) as the origin, the Cartesian coordinate system is established, and the arc center is determined according to the tangent line perpendicular to the port of the slip plane. Then, the value of the overall stability safety factor of the slope is the ratio of the anti-sliding moment to the sliding moment on the potential sliding arc. Figure 7 shows the calculation diagram.

In Figure 7, O_1 is the center of the arc surface, R_1 is the arc radius, q_i is the additional stress, b_i is the i band width, h_i is the i band height, w_i is the soil weight of the i band, l_i is the i band bottom length, β_j is the inclination of the j layer anchor, α_i is the angle between the tangent point of the strip and the arc to the center edge line and the vertical line, and h is the length of the supporting pile.

3.3 Establishment of parameters

- 1) Determination of the internal force of the top beam and anchor

The internal forces of the top beam and anchor can be solved using Eqs 1, 16 of the matrix stiffness equation mentioned above.

- 2) Calculation of the antislide moment of the supporting pile

$$M_p = R \cos \alpha_i \sqrt{\frac{2M_c \gamma h_i (k_p - k_a)}{d + \Delta d}} \quad (21)$$

where M_p is the anti-slide moment produced by the middle pile per meter, R is the arc radius, α_i is the angle between the tangent point of the strip and the arc to the center of the circle and the vertical line, M_c is the bending moment of each pile, h_i is the depth from the arc surface to the slope, γ is the weight of soil within the range of h_i , k_p and k_a are the passive and active earth pressure coefficients of soil, respectively, d is the pile diameter, and Δd is the net spacing between the two piles.

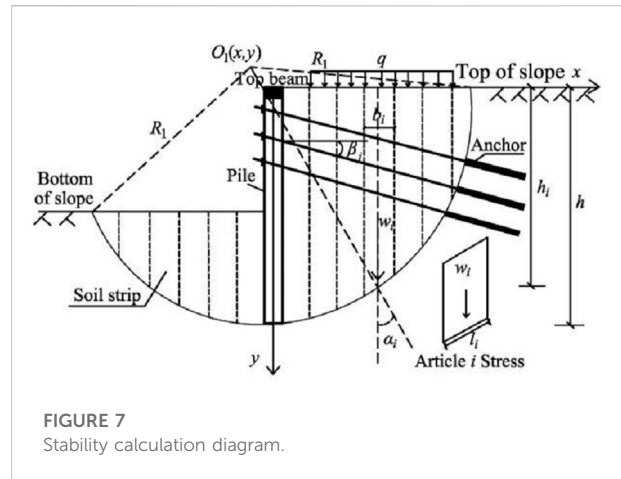


FIGURE 7
Stability calculation diagram.

3.4 Calculation of overall stability of slope

The main difference in stability between the slope supported by the top beam combined with the pile and anchor and the ordinary slope is that when the slip surface passes through the anchor and supporting pile, supporting structures such as the top beam, supporting pile, and anchor will provide tensile moment and anti-sliding moment.

The anti-sliding moments M_{ri} , M_{si} , and M_S produced by the bolt and the anti-sliding moment M_B produced by the top beam on the sliding arc slope of the i th strip are expressed, respectively, as follows:

$$M_{ri} = \sum [(w_i + q_i b_i) \cos \alpha_i \tan \varphi_i + c_i l_i] R \quad (22)$$

$$M_{si} = \sum (w_i + q_i b_i) \sin \alpha_i R \quad (23)$$

$$M_S = \frac{\sum [F_{Tj} \sin(\theta_j + \beta_j) \tan \varphi_i + F_{Tj} \cos(\theta_j + \beta_j)] R}{S_{hj}} \quad (24)$$

$$M_B = \frac{T_k y_0 + M_k}{S_p} \quad (25)$$

The overall stability safety factor of the slope support system is as follows:

$$F_S = \frac{M_{ri} + M_p + M_S + M_B}{M_{si}} \quad (26)$$

where w_i is the soil weight of the soil strip i , l_i is the length of the bottom surface of the soil strip, c_i and φ_i are the cohesion and internal friction angle of the soil layer where the circular sliding surface of the soil strip is located, F_{Tj} is the tension provided by the j th row of anchors, S_{hj} is the horizontal spacing of the j th row of anchors, S_p is the horizontal spacing of the adjacent supporting piles, θ_j is the angle between the j th row anchor axis and the tangent of the failure surface, T_k is the shear force produced by the top beam at the top of the k th pile, y_0 is the vertical distance from the

circle center to the horizontal plane at the pile top, and M_k is the bending moment produced by the top beam at k th pile top.

4 Example analysis

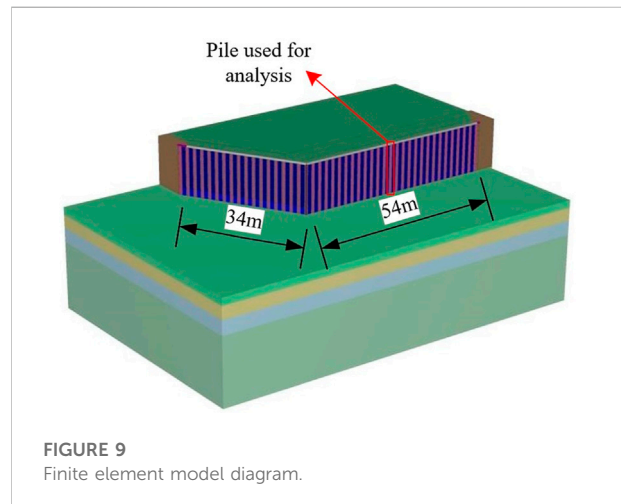
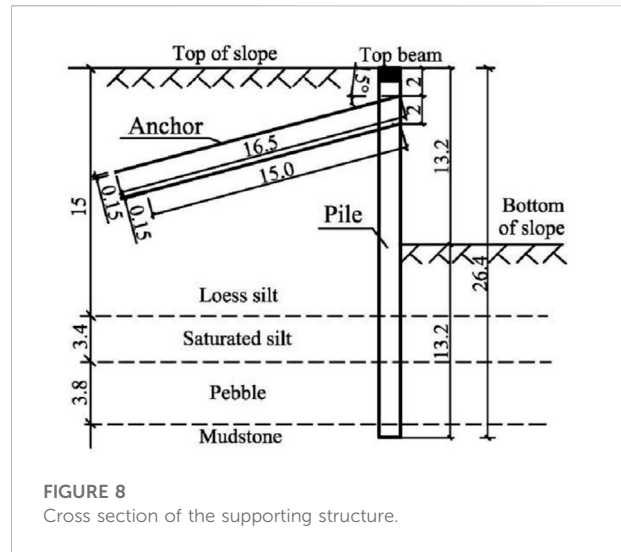
4.1 Project overview

Consider, for example, the slope support project of a crown-beam synergistic pile–anchor structure in Gansu Province, China. A slope with a length of nearly 120 m needs to be supported on the southeast side of the site. The diameter of the supporting pile is 1,500 mm, the distance between piles is 2,000 mm, the length is 26.4 m, the embedded depth is 13.2 m, and the concrete strength grade of the pile body is C40. The anchor adopts an HRB400 Φ 32 mm steel bar as the main reinforcement, which is located at 2 and 4 m below the pile top. The lengths are 16.5 and 15 m, respectively. The inclination angle is 15° , the anchor diameter is 150 mm, the horizontal spacing of the anchor is 2 m, and the designed pulling force is 110 kN. The section size of the top beam is width \times height = 1.5 m \times 0.8 m, and the strength grade is C40. Figure 8 shows the support scheme.

4.2 Establishment of the PLAXIS 3D finite element model

The three-dimensional numerical model of the slope is established using PLAXIS 3D finite element software, and the internal force and displacement of the slope supported by the top beam combined with the pile–anchor structure are calculated. The two sides of the slope are at an angle of 120° , and the lengths of the two sides are 34 and 54 m, respectively. The boundary condition of the model is set according to the actual state of the slope. The upper boundary is free, the surrounding boundary is normally fixed, and the bottom boundary is completely fixed. The distance between the supporting pile and the outer boundary of the slope should be three times or more the height of the slope, and the vertical boundary should be two times or more the height of the slope to avoid the boundary adverse effect on the slope and supporting structure. Usually, the bottom should be taken into hard rock. The dimension of the finite element model is $x \times y \times z = 80 \text{ m} \times 105 \text{ m} \times 40 \text{ m}$. Figure 9 shows the model diagram.

The slope support model of the pile–anchor structure with and without a top beam is established, and Table 1 shows the soil parameters. The soil material simulation uses the soil hardening model (referred to as the HS model). In conventional geotechnical engineering numerical analysis, the soil deformation results obtained using the HS model are most consistent with engineering practice and are significantly better than those of other soil constitutive models. In the numerical simulation, the mesh sparse density is set to “fine,”



which is divided into 2,30,447 elements and 3,20,183 nodes, and the relative element size is 0.7 m.

The material model of the slope supporting structure is linearly elastic, the pile and full-length anchor are simulated by an embedded beam element (embedded pile), the top beam structure is simulated by a beam element, and the concrete baffle is simulated by a plate element. The interface element is established to simulate the interaction between the pile and soil, and the interface is selected as “partially rough.” Table 2 shows the structural design parameters. When the numerical simulation divides the grid, the grid sparse density is set to “fine.” Concurrently, the grid within a certain range of the supporting structure is encrypted, and a fine and accurate grid is generated for the parts where large concentrations or large deformations may occur. A total of 77,196 elements and 1,17,771 nodes are divided.

TABLE 1 Soil parameter table.

Soil layer		Loess silt	Saturated silt	Pebble	Mudstone
Thickness/m		15	3.4	3.8	17.8
Severe $\gamma/(kN/m^3)$		15.7	18.7	24	18
Compression modulus (<i>Mpa</i>)	<i>E₅₀^{refa}</i>	9.3	4.8	50	20.7
	<i>E_{oed}^{refb}</i>	9.3	4.8	50	20.7
	<i>E_{ur}^{refc}</i>	32.5	17.8	150	62.1
Cohesion <i>c/kpa</i>		15	18	5	25
Frictional angle $\varphi/(\circ)$		22	24	28	35

^aThe meaning of the italics is "Secant stiffness"

^bThe meaning of the italics is "Tangent stiffness"

^cThe meaning of the italics is "Unloading/loading stiffness"

TABLE 2 Structural design parameter table.

Envelope structure	Piles	Top beam	Anchor	Retaining plate
Structural model	Embedded beam element	Beam element	Embedded beam element	Plate element
Severe $\gamma/(kN/m^3)$	25	25	25	15.5
Compression modulus <i>E/(Gpa)</i>	32.5	32.5	32.5	30
Poisson ratio	0.2	0.2	0.2	0.15

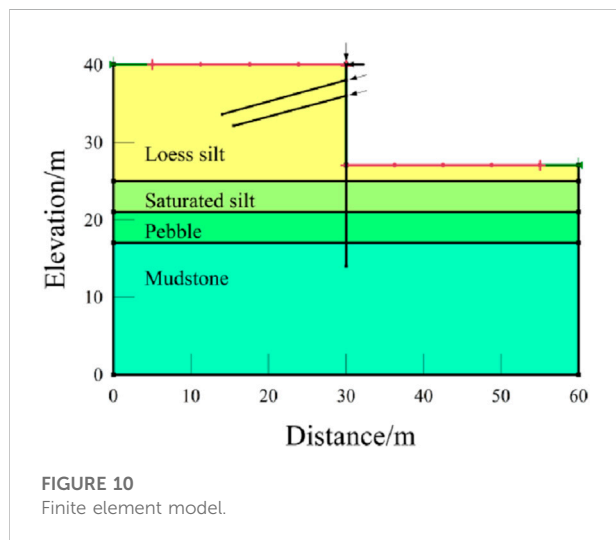


FIGURE 10 Finite element model.

4.3 Establishment of the GeoStudio slope model

The analysis model is established in the SLOPE/W module of GeoStudio. The Morgenstern–Price method is used for slope stability analysis, and the semisine function is selected as the conditional force function. The constitutive relation of soil adopts the Mohr–Coulomb ideal elastic–plastic model, and the parameters of soil and the supporting structure are inputted according to the

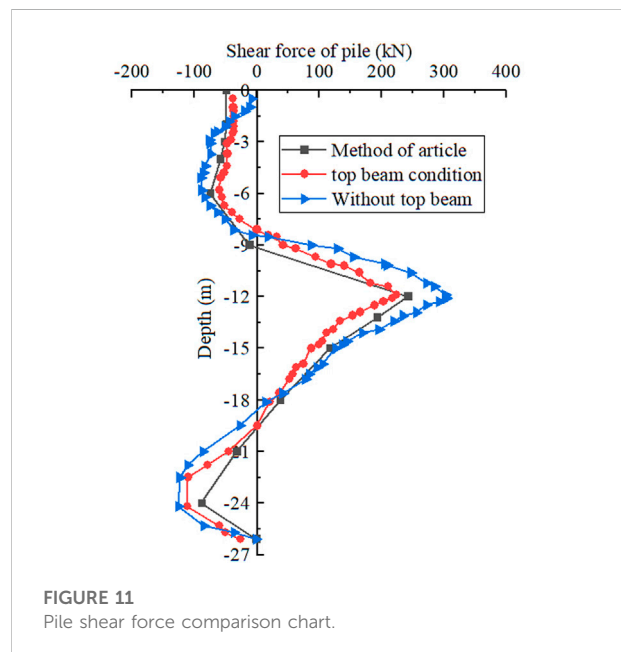
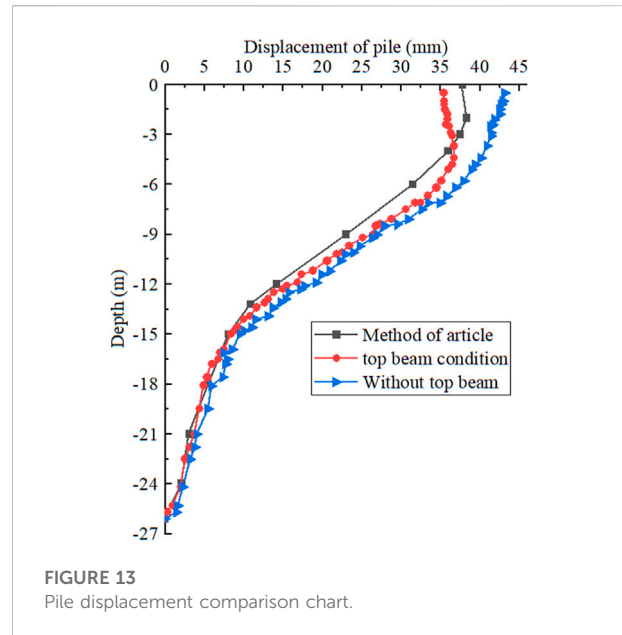
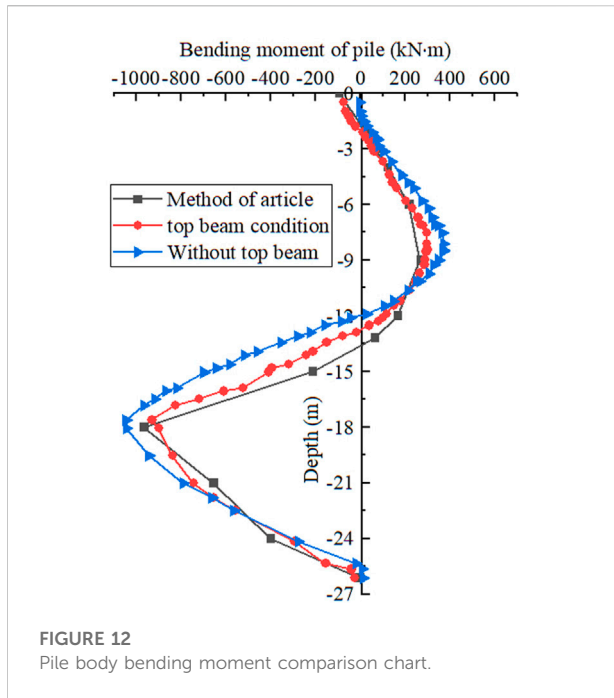


FIGURE 11 Pile shear force comparison chart.

parameters in Tables 1 and 2. The supporting pile and fully bonded anchor are added by strengthening the load, and the internal force of the top beam is added to the pile top according to the point load. Figure 10 shows that the size of the GeoStudio finite element model is $x \times y = 60 \text{ m} \times 40 \text{ m}$.



5 Calculation results and analysis

The specific parameters of the project are substituted into the program compiled by MATLAB; the shear force, bending moment, displacement, and minimum safety factor of the slope are calculated; and the results are compared with the simulation results of PLAXIS 3D and GeoStudio software.

5.1 Analysis of the internal force and deformation of a slope supported by a crown-beam cooperative pile–anchor structure

5.1.1 Comparative analysis of the shear force of the pile

From the shear curve of the pile in Figure 11, the calculation results of this method are consistent with the overall stress of the top beam, which verifies the rationality of this method. Under the constraint of the top beam, the shear force at the pile top is similar, but under the condition of no top beam, the shear force at the pile top is -9.78 kN . At the maximum positive shear force of the pile, the maximum shear force calculated by this method and that under the condition of the top beam are 346.81 and 320.4 kN , respectively, which differ from the maximum shear force of the nontop beam. The comparison of the shear force between the pile top and the maximum positive shear force of the pile shows that the top beam can prevent the pile from developing to an empty surface.

5.1.2 Comparative analysis of the bending moment of the pile body

From the comparison diagram of the bending moment of the pile body in Figure 12, the bending moment value obtained by this method is similar to that of the bending moment curve with and without the top beam. However, at the position of the pile top, the bending moment of the nontop beam starts to change from zero, whereas the bending moment at the pile top is -92.21 kN m calculated by this method, and it is -73.92 kN m under the condition of the top beam, indicating that the existence of the top beam can effectively enhance the stress state of the pile top. The maximum positive and negative moment values appear near the buried depth of -9 and -18 m , and the comparison of the working conditions with and without the top beam shows that the existence of the top beam effectively reduces the bending moment of the pile.

5.1.3 Comparative analysis of pile displacement

From the variation curve of pile displacement in Figure 13, the method presented in this study is similar to the variation law of pile displacement under the conditions of crown and nontop beams. The calculation result of this method is smaller than that of the top beam as a whole, but the existence of the top beam induces a large difference between the crown and nontop beams at the pile top, and the maximum reaches 5.87 mm , which shows that the top beam can connect both sides of the pile to make the top beam and pile deformation, thus reducing the displacement of the pile top and improving the overall stability of the supporting structure.

5.2 Overall stability analysis of a slope supported by a top beam combined with a pile–anchor structure

On the basis of the calculation and analysis of the above engineering examples, using the overall stability calculation method in this study, the minimum safety factors of the pile–anchor structure supporting slope with and without a top beam are 1.432 and 1.356, respectively, whereas the minimum safety factors of overall stability with and without a top beam cooperative support obtained by GeoStudio simulation are 1.413 and 1.340, respectively. By comparison, it is found that the calculation result of this method is similar to that obtained by numerical simulation, and the overall safety factors of the slope supported by a top beam and a pile–anchor structure are increased by 5.60% and 5.44%, respectively. Hence, the existence of the top beam significantly improves the overall stability; that is, the safety of the slope is significantly improved.

6 Conclusion

In this study, a simplified calculation method for solving the internal force and displacement of supporting structures and the overall stability of the slope was proposed by establishing the calculation model of stress deformation and the overall stability of the slope supported by a top beam combined with a pile and an anchor. By taking a slope project of a crown-beam cooperative pile–anchor support as an example, this method was compared with the numerical simulation with and without a crown-beam cooperative support, and the following conclusion are obtained.

- (1) According to the deformation coordination principle of the pile–anchor structure at the pile top and anchor end, the integral matrix equation was established by dividing the supporting pile into finite elements, and the calculation expressions of shear force, bending moment, and pile displacement of the supporting pile were obtained.
- (2) On the basis of the Swedish slice method, an overall stability analysis of the slope supported by a top beam and pile–anchor was conducted, and the calculation method of the minimum safety factor of the overall stability of the slope was obtained.
- (3) The internal force and displacement values calculated by this method were compared with the internal force distribution and deformation values obtained by PLAXIS 3D numerical simulation, and the law was similar. In addition, the slope overall stability coefficient calculated by this method was compared with that obtained by GeoStudio numerical analysis, and their values were close, thereby confirming the rationality of the proposed method.
- (4) The numerical simulation results of crown and nontop beams showed that the existence of a top beam can effectively

improve the anti-deformation ability of pile, which can more effectively control slope deformation and can increase its overall stability coefficient. As a result, the anti-sliding ability and safety stability of the slope are improved.

Data availability statement

The original contributions presented in the study are included in the article/supplementary material, further inquiries can be directed to the corresponding author.

Author contributions

TM and SY completed the drafting of the original paper, and YZ made important revisions to the paper. All authors participated in the theoretical research derivation and numerical simulation modeling work of the paper.

Funding

This work was supported by the National Natural Science Foundation of China (Grant No. 52068048) and the Natural Science Foundation of Gansu Province, China (Grant No. 20JR10RA163).

Acknowledgments

The corresponding author would like to acknowledge the National Natural Science Foundation of China (Grant No. 52068048) and the National Natural Science Foundation of Gansu Province, China (Grant No. 20JR10RA163). The financial supports are gratefully acknowledged.

Conflict of interest

The authors declare that the research was conducted in the absence of any commercial or financial relationships that could be construed as a potential conflict of interest.

Publisher's note

All claims expressed in this article are solely those of the authors and do not necessarily represent those of their affiliated organizations, or those of the publisher, the editors and the reviewers. Any product that may be evaluated in this article, or claim that may be made by its manufacturer, is not guaranteed or endorsed by the publisher.

References

- Bai, B., Wang, Y., Rao, D., and Bai, F. (2022). The effective thermal conductivity of unsaturated porous media deduced by pore-scale SPH simulation. *Front. Earth Sci. (Lausanne)*. 10, 943853. doi:10.3389/feart.2022.943853
- Bai, B., Yang, G., Li, T., and Yang, G. (2019). A thermodynamic constitutive model with temperature effect based on particle rearrangement for geomaterials. *Mech. Mater.* 139, 103180. doi:10.1016/j.mechmat.2019.103180
- Bai, B., Zhou, R., Cai, G., Hu, W., and Yang, G. (2021). Coupled thermo-hydro-mechanical mechanism in view of the soil particle rearrangement of granular thermodynamics. *Comput. Geotechnics* 137, 104272. doi:10.1016/j.compgeo.2021.104272
- Cai, F., and Ugai, K. (2011). A subgrade reaction solution for piles to stabilise landslides. *Geotechnique* 61 (2), 143–151. doi:10.1680/geot.9.p.026
- Chen, W. X., Guo, Z. K., and Zhang, W. G. (2006). A calculation method for the internal force and deformation of row piles considering the action of ring beam. *Chin. J. Undergr. Space Eng.* 411–415. (in Chinese).
- Chen, F. Y., Zhang, R. H., Wang, Y., Liu, H. L., Böhlke, T., and Zhang, W. G. (2020). Probabilistic stability analyses of slope reinforced with piles in spatially variable soils. *Int. J. Approx. Reason.* 122, 66–79. doi:10.1016/j.ijar.2020.04.006
- Di, P. C., Galli, A., Aversa, S., and Maiorano, R. M. S. (2018). “Multi-level design approaches for slope-stabilizing piles,” in *Volume 1-3 of landslides and engineered slopes: Experience, theory and practice*. Editors S. Aversa, L. Cascin, L. Picarelli, and C. Scavia (London: CRC Press), 1–3, 821–826. doi:10.1201/9781315375007-86
- Ding, M., and Zhang, Y. X. (2012). Analysis method of pile-anchor structure based on matrix displacement method. *Eng. Mech.* 29 (8), 116–122. (in Chinese). doi:10.6052/j.issn.1000-4750.2010.11.0858
- Dong, X. G., Zheng, L. I., Cui, Z., and Zhou, C. (2022). Stability analysis of the pile-prestressed anchor composite structure based on failure mode. *Eng. Fail. Anal.* 137, 106223. doi:10.1016/j.engfailanal.2022.106223
- Huang, C., Ren, W., and Kong, L. (2013). New mathematical modelling of stabilizing pile with prestressed tieback anchors. *Math. Problems Eng.* 2013, 1–12. doi:10.1155/2013/601508
- Kang, G. C., Song, Y. S., and Kim, T. H. (2009). Behavior and stability of a large-scale cut slope considering reinforcement stages. *Landslides* 6 (3), 263–272. doi:10.1007/s10346-009-0164-5
- Li, X. C. (2011). “Large-scale physical model test study on the interaction between landslide and anchor anti-slide pile,” (Xi’an: Chang’an University). Dissertation (in Chinese).
- Li, Y., and Zhang, W. (2020). Investigation on passive pile responses subject to adjacent tunnelling in anisotropic clay. *Comput. Geotechnics* 127, 103782. (in Chinese). doi:10.1016/j.compgeo.2020.103782
- Prat, P. C. (2017). Numerical investigation into the failure of a micropile retaining wall. *Comput. Geotechnics* 81, 262–273. doi:10.1016/j.compgeo.2016.08.026
- Satvati, S., Alimohammadi, H., Rowshanzamir, M., and Hejazi, S. M. (2020). Bearing capacity of shallow footings reinforced with braid and geogrid adjacent to soil slope. *Int. J. Geosynth. Ground Eng.* 6 (4), 41–12. doi:10.1007/s40891-020-00226-x
- Shu, J., and Zhang, D. (2017). A case study: Observed deformation characteristics and internal force of pile-anchor retaining excavation. *Geotech. Front.* 136–148. doi:10.1061/9780784480458.014
- Smethurst, J. A., and Powrie, W. (2007). Monitoring and analysis of the bending behaviour of discrete piles used to stabilise a railway embankment. *Geotechnique* 57 (8), 663–677. doi:10.1680/geot.2007.57.8.663
- Song, H., and Cui, W. (2016). A large-scale colluvial landslide caused by multiple factors: Mechanism analysis and phased stabilization. *Landslides* 13 (2), 321–335. doi:10.1007/s10346-015-0560-y
- Sun, J., Wang, S., Shi, X., and Zeng, L. (2019). Study on the design method for the deformation state control of pile-anchor structures in deep foundation pits. *Adv. Civ. Eng.* 2019, 1–16. doi:10.1155/2019/9641674
- Suo, W. B., Gang, C., Lu, Y., Sun, Y. J., and Shi, B. (2016). Study on distributed monitoring method of deep foundation pit retaining pile based on the Brillouin optical time domain technology. *Geol. J. China Univ.* 22 (4), 724–732. (in Chinese). doi:10.16108/j.issn1006-7493.2016165
- Wang, D. Q., and Zhu, Y. P. (2014). Additional stress apply to analyzing the stability of prestressed anchor support. *Eng. Mech.* 31 (4), 196–202. (in Chinese). doi:10.6052/j.issn.1000-4750.2012.11.0824
- Wang, X., Luo, X. H., Xue, L. W., and Bo, J. (2021). Back analysis of pile and anchor retaining structure based on BOTDA distributed optical fiber sensing technology. *E3S Web Conf.* 248, 01036. doi:10.1051/e3sconf/202124801036
- Ye, S. H., Fang, G. W., and Ma, X. R. (2019). Reliability analysis of grillage flexible slope supporting structure with anchors considering fuzzy transitional interval and fuzzy randomness of soil parameters. *Arab. J. Sci. Eng.* 44 (10), 8849–8857. doi:10.1007/s13369-019-03912-9
- Ye, S. H., and Zhao, Z. F. (2020). Seismic response of pre-stressed anchors with frame structure. *Math. Problems Eng.* 5, 1–15. doi:10.1155/2020/9029045
- Zeng, Q. Y., and Liu, M. C. (1995). Mechanism and calculation analysis of supporting pile ring beam. *Rock Soil Mech.* 16 (2), 74–82. (in Chinese). doi:10.16285/j.rsm.1995.02.009
- Zhang, W., Li, Y., Goh, A. T. C., and Zhang, R. (2020). Numerical study of the performance of jet grout piles for braced excavations in soft clay. *Comput. Geotechnics* 124, 103631. doi:10.1016/j.compgeo.2020.103631
- Zhao, W., Han, J. Y., Chen, Y., Jia, P. J., Li, S. G., Li, Y., et al. (2018). A numerical study on the influence of anchorage failure for a deep excavation retained by anchored pile walls. *Adv. Mech. Eng.* 10 (2), 168781401875677. doi:10.1177/1687814018756775
- Zheng, J., He, H., and Alimohammadi, H. (2021). Three-dimensional Wadell roundness for particle angularity characterization of granular soils. *Acta Geotech.* 16 (1), 133–149. doi:10.1007/s11440-020-01004-9

Nomenclature

Abbreviations

A bolt cross-sectional area

a polar moment of inertia calculation factor for top beams

a_i the angle between the tangent point of the soil strip and the arc to the edge of the circle and the vertical line

b_0 beam element width

b short side of rectangular section of top beam

c_i cohesion

d diameter of pile

E modulus of elasticity of piles or anchors

F_T the tension of the anchor to the pile

G shear modulus of top beams

h_i soil bar height

I moment of inertia of pile section

I_t polar moment of inertia of top beam

k_{si} equivalent stiffness of soil spring

k_{Ti} equivalent stiffness of soil spring

k_a active earth pressure coefficient

k_b passive earth pressure coefficient

L the length of the top beam

l beam element length

l_i the length of the i -th bolt

m horizontal elastic coefficient of foundation

M_k constraint moment of top beam to supporting pile

M_i moment at node i

M_p anti-slide moment produced in pile per meter

M_c bending moment of each pile

M_{ri} anti-slip moment on the slope of the i -th soil strip

M_{si} sliding moment on the slope of the sliding arc of the i -th strip

M_S anti-slip moment generated by anchor

M_B anti-slip moment due to top beam

P pressure strength at any point on the pile

R arc radius

S_h anchor horizontal spacing

S_P support pile horizontal spacing

T_{ki} binding force of top beam to supporting pile

u_{ek} horizontal displacement generated by the k -th pile top

u_{ei} horizontal displacement of pile body under the action of earth pressure alone

w horizontal displacement of pile body

w_i soil strip i with soil weight

z pile length

Greek symbols

θ_j the angle between the axis of the j -th row of anchors and the tangent to the failure surface

γ the weight of soil

θ_{ek} the angle produced by the top of the k -th pile

δ_{ZTk}^u the horizontal displacement at the top of the pile when the horizontal unit force is applied to the top of the k -th pile.

δ_{ZTk}^0 the rotation angle at the top of the pile when the horizontal unit force is used at the top of the k -th pile.

δ_{ZMk}^u the horizontal displacement at the top of the pile when the unit moment acts on the top of the k -th pile.

δ_{ZMk}^0 the rotation angle at the top of the pile when the unit moment acts on the top of the k -th pile.

δ_{P0kFTi}^u the horizontal displacement of the top of the k -th pile when the unit force is used in the i -row anchor of the supporting pile.

δ_{P0kFTi}^0 when the unit force is used in the i -th row anchor of the supporting pile, the rotation angle at the top of the k -th pile

δ_{LFkm}^u the horizontal displacement at point k when the unit force at point m is applied to the top beam.

δ_{LMkm}^0 when the unit force at the m point is applied to the top beam, the rotation angle at the k point occurs

δ_{PiTk}^u the displacement of the k -th pile at the anchor end of the i -th row when there is a horizontal unit force at the top of the pile.

δ_{PiMk}^u the displacement of the pile at the anchor end of the i -th row when there is a horizontal unit moment at the top of the k -th pile.

δ_{PiFTj}^u displacement of supporting pile at the anchor end of row I under the action of unit axial force of j -row anchor

δ_{PiFTi}^u the displacement at the anchor end of the i -th row anchor of the supporting pile under the action of unit axial force.

φ_i internal friction angle